PSEUDO STEADY STATE TECHNIQUE FOR RELATIVE PERMEABILITY MEASUREMENT

by

G. A. Virnovsky, Y. Guo, .K.O. Vatne,
Rogaland Research, Stavanger, Norway,
and E.M. Braun,
Exxon Production Research Co., Houston, USA.

ABSTRACT

A pseudo-steady-state method of measuring relative permeability is described and investigated through both numerical simulation and laboratory experiments. The method is found to be valid over most of the attainable saturation range, and to require significantly less measurement time than the traditional steady-state method.

In steady-state relative permeability measurements, two phases (typically oil and water) are injected into a core sample simultaneously at a series of discrete ratios. Data for relative permeability calculations are taken at equilibrium conditions, when the flow rates of oil and water exiting the core are at the same as those entering the core, and when the pressure drop across the core is constant. In the pseudo-steady-state method, flow rates of oil and water entering the core are changed slowly and continuously. Data for relative permeability calculations are taken under near equilibrium conditions, i.e. flow rates at the core outlet differ slightly from those at the inlet, and the pressure drop is changing slowly.

A method is presented for determining the optimum schedule of flow rate changes for achieving a specified degree of accuracy. This method, based on an assumption of negligible capillary pressure effects, leads to simple criteria for controlling the level of errors in the resulting relative permeability curves. Use of these criteria is demonstrated through numerical simulation. Errors due to lack of equilibrium are found to be small relative to those from capillary pressure effects.

The pseudo-steady-state method is also demonstrated experimentally on a Berea sandstone core. Repeat tests were conducted with three different ramping schedules. The best results were obtained by starting the test with one conventional steady-state data point and continuing with the pseudo-steady-state method.

INTRODUCTION

The conventional steady-state method for two-phase relative permeability measurements is well known [1]. Two phases (usually oil and water) are injected into a core sample simultaneously at a series of ratios, with the total flow rate typically being held constant.

Rates are held constant at each ratio until equilibrium conditions are reached, i.e. until the pressure drop and the effluent flow rates are no longer changing. The need to achieve a series of equilibrium states results in long test times and high cost.

Our practice in some steady-state tests has been to change (ramp) flow rate ratios gradually, rather than suddenly, between the specified values. It has been observed that relative permeability obtained during the gradual changes are nearly as accurate as those obtained under equilibrium conditions, with the exception of data obtained near the endpoint saturations. This observation has led to the current investigation of the pseudo-steady-state method as a means of obtaining accurate data more rapidly than in the conventional steady-state method.

Ramping speed has been found to be the most important parameter in the design of pseudo-steady-state tests. Slow ramping contributes to more accurate relative permeability results, since conditions in the core are closer to equilibrium. Fast ramping, however, reduces experimental time and cost. To achieve a proper balance between accuracy and cost, it is important to determine the maximum ramping speed for a given level of accuracy.

THEORY

The optimal ramping speed depends on the properties of the porous medium and the fluid system, i.e. relative permeabilities which are not known before the experiment. Therefore, it is necessary to express the ramping speed in terms of a quantity which can be observed and controlled. We choose this quantity to be the difference between fractional flows at the injection and production ends of the core:

$$f^{\text{inj}}(Q) - f^{\text{prod}}(Q) = \gamma$$

where γ is the "accuracy parameter". If γ is kept constant in time, then from mass conservation it follows that the average saturation in the core changes linearly with time. In addition, if γ is small enough the deviation of the saturation in the core from the average value will also be small. Therefore the saturation at the core inlet will be close to the average, i.e. it will also change linearly with time. From this it immediately follows, that the water fractional flow at the inlet should vary in a manner that reproduces the shape of the fractional flow vs. saturation curve. More precisely, the following equation describes the optimal ramping path

$$f(Q) = \overline{\varphi}(Q\frac{\gamma}{v}), \qquad v = V(1 - S_{wi} - S_{or}), \quad \overline{\varphi}\left(\frac{S_w - S_{wi}}{1 - S_{wi} - S_{or}}\right) = \varphi(S_w), \tag{1}$$

where $f(Q)$ is the fractional flow as a function of the total fluid volume injected, v the effective pore volume, and $\bar{\varphi}$ is the fractional flow as a function of normalised saturation. Eq.(1) describes the optimal ramping path and its dependence upon the accuracy parameter, γ. Since the curve describing fractional flow as a function of saturation is typically not a straight line, the optimal ramping path is non-linear: ramping speed is relatively slow near end point saturations and faster at intermediate saturations. The appendix provides a complete error analysis of this method.

NUMERICAL SIMULATIONS

The simulations are performed using CENDRA [2], a core flood simulator. Simulation parameters were adjusted, so that the numerical errors were small compared to laboratory measurements uncertainty in the following way: (1) solution tolerance for the oil pressure was 0.005 KPa, (2) solution tolerance for the water saturation was 10^{-6}, and (3) one hundred grid blocks were used to avoid significant numerical dispersion.

In the simulation, the pressure at the core outlet was held constant, and the injection rates varied according to the ramping path. Table 1 shows the input relative permeability curves which are based on North Sea reservoir data. For the first case, input capillary pressure was zero at all values of water saturation. Then for a given value of γ, fractional flow can be calculated from eq.(1); with this value of fractional flow, oil and water flow rates can be calculated for a ramping schedule.

Simulated results of one pseudo-steady-state test with γ=0.01 are shown in Figure 1. Except for the initial and final times, the non-linear ramping path gives a linear change of the average water saturation in the core

The water saturation profiles (see Figure 2, solid line) are non-constant before breakthrough, and are quite constant thereafter. Figure 3 compares input relative permeabilities with those calculated from the simulated pseudo-steady-state experiment. The two sets of curves match closely. Next capillary pressure was added to the simulation. An analytical capillary pressure curve, given by

$$P_c = 187.5\left(S_w^* - S_{wp}^*\right)\left[\left(S_w^* - b\right)^2 + c\right] \quad where \;\; b = 0.7,\; c = 0.0433.$$

was used as the input. Here the constants b and c are chosen to give zero capillary pressure at a water saturation 0.5, an inflection point in the curve at a water saturation of 0.6, and maximum and minimum capillary pressures of 80 and -3.0 KPa.

Capillary pressure acts to diffuse the water saturation profile before breakthrough (see Figure 2) because the water spontaneously imbibes ahead of the front. Nonetheless, the breakthrough time is not far different from that for the zero capillary pressure case. After breakthrough, the water saturation profiles are not constant as they were in the zero capillary pressure case. Figure 3 shows that relative permeability curves calculated from the pseudo-steady-state simulation (with non-zero capillary pressure) do not match the input curves as well as in the first case.

DISCUSSION OF ERRORS

There are at least two sources of error in relative permeabilities calculated from the pseudo-steady-state test: (1) error due to ramping, or the effect of having a time-varying water saturation in the core (hence, injection and production rates are not equal), and (2) error due to neglect of the capillary pressure, or the effect of having a spatially-varying water saturation in the core (even when injection and production rates are equal).

Error due to ramping

Error in total mobility in the ideal cases (zero capillary pressure) can be calculated analytically from Eq. A3, and is a function of, among other parameter, the total mobility and ramping speed. Figure 5 compares the error in total mobility for the different ramping speeds ($\gamma = 0.01$, 0.02, 0.05 and 0.1). The errors in total mobility are calculated from the difference between the input relative permeability curves for the simulation and the calculated ones directly from Darcy's equations using the output pressure drop, oil production and the production rates at outlet end. The error is negative in the regions close to S_{wi} and S_{or}, and is positive in the intermediate saturation range. As shown in Figure 5, the error can be significantly reduced by increasing the ramping period. Generally, the error in the idealised cases is small (with γ=0.01 it is less than 1% of effective permeability in order) compared to the other possible experimental errors, and can be accepted.

Errors due to neglecting capillary pressure

The errors in the pseudo-steady-state relative permeabilities are very much influenced by the capillary effect. In general, the error at low saturations is caused by the delay of break through and the non-uniform water saturation after break through. In addition, if the forced imbibition capillary pressure is high, as for weak water-wet and mixed-wet cases, the water saturation is not uniform at equilibrium causing a large error at high water saturation. The level of error is considerably higher than that caused by the pseudo-steady-state condition when capillary pressure is zero, as shown in Figure 6. However, since the water saturation profiles are affected by the capillary pressure not only at the transient period, but also at the equilibrated stage, the payoff from the elongated ramping period is not necessarily obvious. This is demonstrated by Figure 3 where both pseudo-steady-state and steady-state relative permeability curves are plotted. As one can see, the steady-state relative permeabilities are equally affected by the capillary effect. Figure 3 also suggests better results from pseudo-steady-state test than the steady-state for the saturations around the water break through for some reason.

Averaging Production and injection rates to minimize error

One possible way to reduce the error due to ramping is to use average of injection and production rates in Darcy's equation. (Experimentally, only injection rates are measured directly, while production rates are calculated from cumulative production data.) Figure 4 shows relative permeabilities calculated from the non-zero capillary pressure case results using the (1) production rate, (2) average rate, and (3) injection rate. In this

specific case, the oil relative permeability curve has least error when calculated with (1), next least with (2), and worst error with (3). For the water relative permeability, the order is the reverse. This reversal in ordering is caused by the imbibition process: the water rate is largest at the inlet face and the oil rate is largest at the outlet face.

EXPERIMENTAL DATA

We performed one steady-state test and three pseudo-steady-state tests on a Berea sandstone core in a five-cylinder recirculating system. The system and experimental procedure are described in Reference [3]. Table 1 gives sample and fluid properties.

Repeat tests were conducted with three different ramping schedules, as shown in Figure 7; Figure 7 also gives the rate schedule for the steady-state portion of the tests. The total injection rate was 2.0 ml/min for all tests.

As depicted in Figure 7, we began the tests with a conventional imbibition steady-state test (SSI) with six different water fractional flow rates. Next, the core was brought back to low water saturation by flooding with oil and from this point we ran the first pseudo-steady-state test (PSSI-1). This cycle of oil flooding followed by a pseudo-steady-state test was repeated for a total of three tests. Test PSSI-2 was a combination of one steady-state point (yielding a water saturation of about 42%) followed by a pseudo-steady-state test with γ=0.01. Similarly, Test PSSI-3 was a combination of one steady-state point (yielding a water saturation of about 37%) followed by a pseudo-steady-state test with γ =0.02. Choice of the ramping path was guided by the results of the steady-state test.

Figure 8 shows the relative permeability curves obtained in each of the tests. Test PSSI-2 gave the best results. Test PSSI-3 had a ramping speed that was too fast; Test PSSI-1 began at a water saturation that allowed ramping rate and capillary pressure effect errors to dominate the results at low values of water saturation (to about 50%). Hence the best results were obtained by starting the test with one conventional data point and continuing with the pseudo-steady-state method.

CONCLUSIONS

1. The pseudo-steady-state method reduces the time required to obtain relative permeabilities as compared to the conventional steady-state method, and gives results that are valid.

2. Best results are obtained with a combination of the conventional steady-state technique (near end-point saturations) and the pseudo-steady-state technique.

3. The optimal ramping speed schedule for a pseudo-steady-state test is non-linear: slow near end-point saturations and faster at intermediate saturations.

4. The error in total mobility, obtained from pseudo-steady-state derived relative permeability curves, is largest near end-point saturations and is near zero at intermediate saturations.

5. Capillary pressure can have a significant effect on the error in relative permeabilities calculated from pseudo-steady-state tests.

6. The difference between the inlet and outlet fractional flow rates can be used to determine the accuracy of the pseudo-steady-state test.

TABLES AND FIGURES

Table 1: Data for BASE CASE used in the numerical simulations

GENERAL DATA:		ROCK CURVES:	
Core length	18.8 cm	Kr correlation	Corey correlation
Core cross section	10.64 cm^2	End-point K_{ro}	1.00
Core porosity	27.0 %	End point K_{rw}	0.716
Core pore volume	54.01 cm^2	S_{wi}	0.20
Absolute permeability	497.7 mD	S_{or}	0.15
Water viscosity	1.00 cp	Corey exponent for water:	2.0
Oil viscosity	2.00 cp	Corey exponent for oil	2.0
Total injection rate	2.0 ml/min	Capillary pressure	None

Table 2 - Berea core sample and fluids used in the experiments

Core length	28.8 cm
Core cross section	10.64 cm^2
Core porosity	22%
Core pore volume	67.62 cm^3
Effective oil permeability (K_{ro} at S_{wi})	485 mD
Oil viscosity	1.10 cp
Water viscosity	1.02 cp

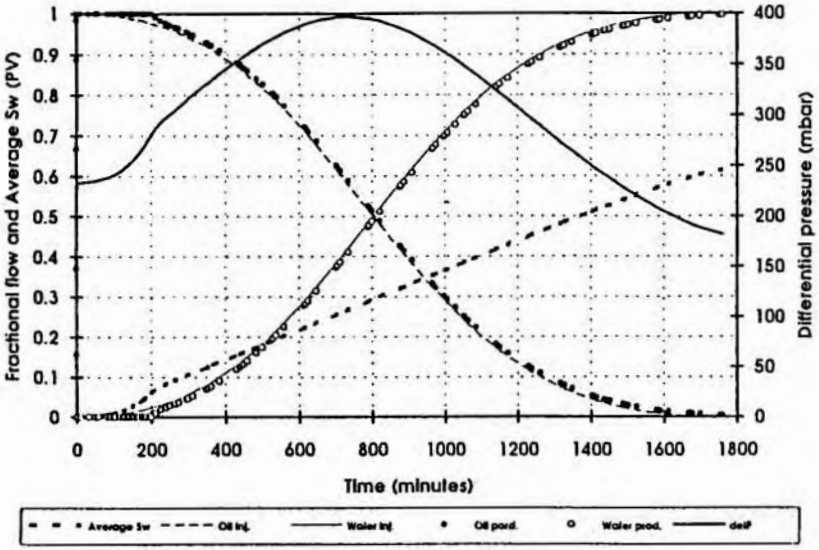

Figure 1 - Simulated pseudo-steady-state experiment.

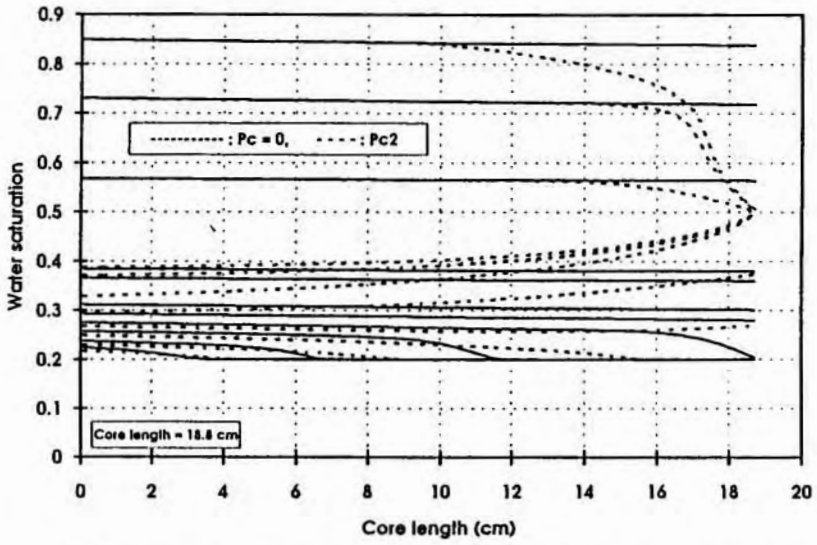

Figure 2 - Water saturation profiles in the ramping period.

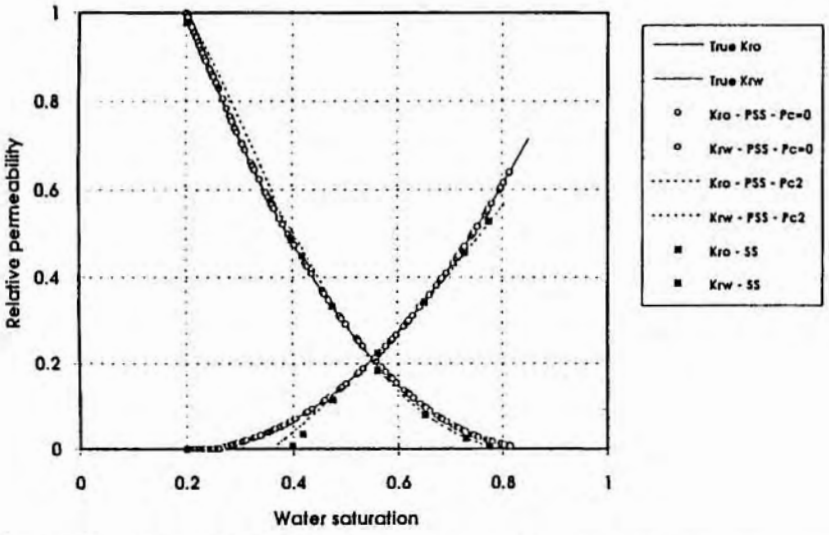

Figure 3 - Relative permeability curves from steady- and pseudo-steady-state flooding.

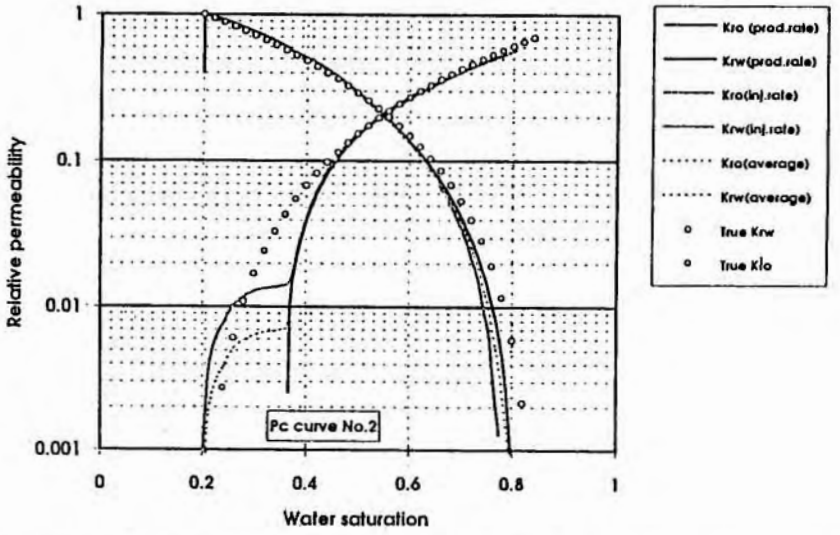

Figure 4 - Relative permeability curves from pseudo-steady-state experiment using various rate data

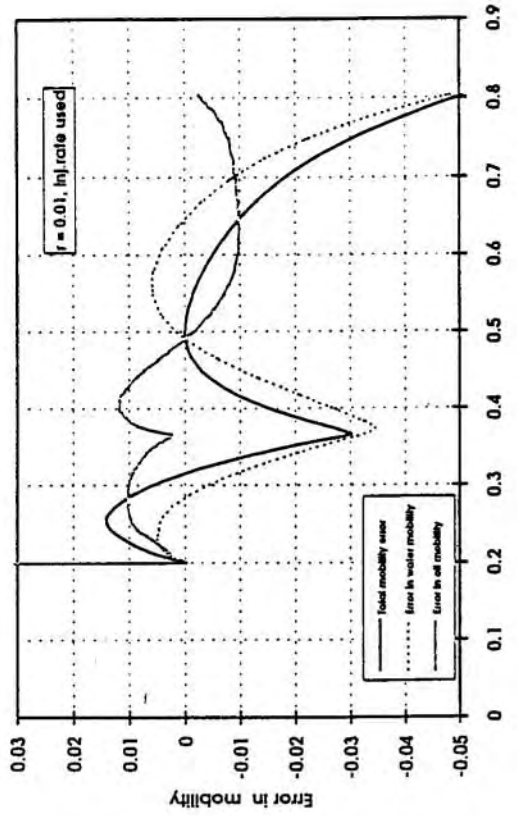

Figure 6 - Error due to capillary pressure effect.

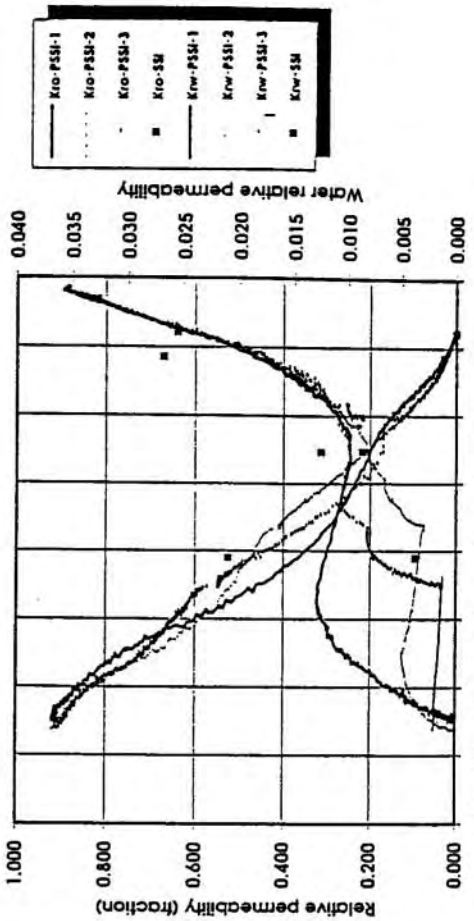

Figure 8 - Relative permeability curves from steady- and pseudo-steady-state experiments.

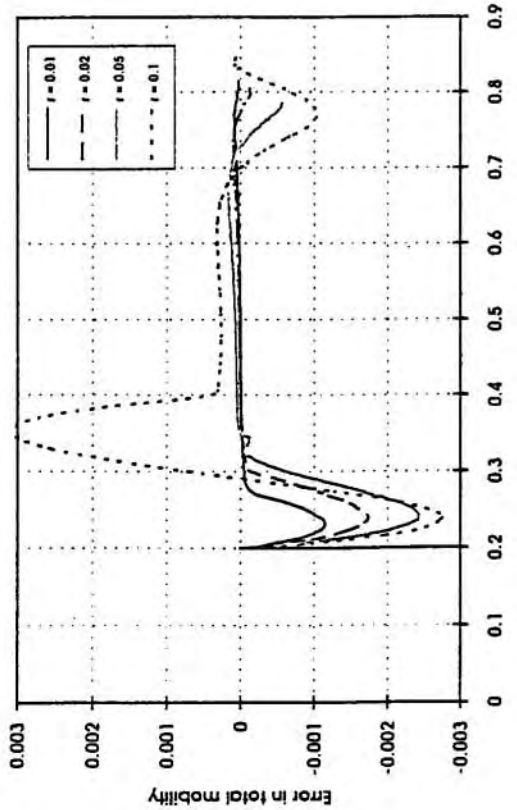

Figure 5 - Error due to ramping speed.

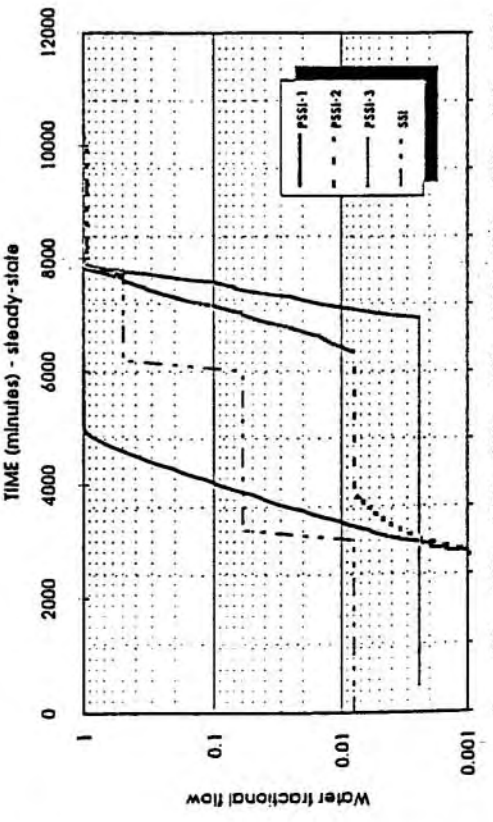

Figure 7 - Ramping paths for the laboratory pseudo-steady-state experiments.

NOMENCLATURE

f	Water fractional flow at the inlet end
k	Absolute permeability
L	Length of core
S	Water saturation
$\overline{S}$	Average water saturation
S^*	Normalised water saturation
P	Pressure
q	Total injection rate
Q	Dimensionless time
t	Time
u	Darcy velocity
V	Pore volume
v	Effective pore volume
x	Coordinate
γ	Dimensionless accuracy parameter
Δ	Increment
λ	Mobility
σ	Standard deviation
φ	Fractional flow
ϕ	Porosity

Subscript

c	Capillary
or	Residual oil
t	Total
wi	Initial water
w	Water

REFERENCES

1. Edward M. Braun and Robert J. Blackwell: "A Steady-State Technique for Measuring Oil-Water Relative Permeability Curves at Reservoir Conditions", SPE 10155, presented at SPE annual meeting in San Antonio, Texas, October 5-7, 1981

2 Ying Guo, Jan-Erik Nordtvedt and Henning Olsen: "CENDRA+ User's manual, version 2.3/3.3", report RF-183/93, 1993.

3. Guo, Y. and Vatne, K.O.: "Use of A New Generation Recirculation System for Steady-State Relative Permeability Measurements", Proceedings of the 7th European Symposium on Improved Oil Recovery, Moscow, Russia, October 27-29, 1993, vol.1, 161.

APPENDIX

Error analysis

Let us estimate the error in a phase mobility resulting from non-uniformity of saturation in the core. For the pseudo-steady state technique phase mobilities are calculated exactly as for the conventional steady state technique, i.e. using the Darcy' formula:

$$\tilde{\lambda}_i = \frac{\tilde{u}_i L}{\Delta\tilde{p}k} = \tilde{f}_i \frac{u_t L}{\Delta\tilde{p}k}, \quad i = w,o \tag{A1}$$

where tilde signifies measured quantities containing errors due to the fact that the saturation is not constant along the core. The input data from laboratory measurements

are: (1) Average saturation in the core; (2) Total pressure drop across the core; (3) Phase velocity.

From the Darcy' law it follows

$$\left(\frac{u_t L}{\Delta\tilde{p}k}\right)^{-1} = \frac{1}{L}\int_o^L r(S(x,t))dx, \qquad r(S) = \frac{1}{\lambda_t(S)}. \tag{A2}$$

Further we use perturbation theory methods assuming small deviations of the saturation from the average value. Assuming deviation of saturation from average to be small, and expanding non-linear function $r(S)$ into series in the vicinity of the average saturation one obtains the following expression for the errors in phase mobilities

$$\Delta\lambda_i(\bar{S}) = \lambda_t(\bar{S})\Delta f_i + f_i(\bar{S})\left[\lambda_t''(\bar{S}) - 2\frac{\lambda_t'^2(\bar{S})}{\lambda_t(\bar{S})}\right]\frac{\sigma^2}{2}, \quad i = w,o.$$

$$\text{with } \Delta\lambda_i = \tilde{\lambda}_i - \lambda_i, \quad \Delta f_i = \tilde{f}_i - f_i, \qquad \sigma^2 = \frac{1}{L}\int_o^L (S(x,t)-\bar{S})^2 dx, \tag{A3}$$

The first term in the right-hand-side of Eq. (A3) represents the error in a phase mobility due to the error in fractional flow. The second term in the right-hand-side of Eq. (A3) represents the error in a phase mobility due to the error in pressure drop or the error in the total mobility. It can be both positive or negative, its sign depends on the total mobility function since σ^2 is non-negative.

We assume that the difference between injection and production fractional flows is kept small, so that $\gamma \geq \Delta f$, where γ is a small parameter controlling accuracy. Then σ^2 is not constant. In the intermediate saturation range, where fractional flow curve is close to linear $\Delta f = \varphi'(\bar{S})(S-\bar{S})$. Raising to the second power and integration readily give $\sigma^2 \propto \Delta f^2 \propto \gamma^2$, and therefore the second term in eq, (A3) can be neglected.

In the saturation intervals close to residuals the second derivative of the fractional flow curve may not be neglected. In this case we have $\gamma \propto \Delta f = \varphi'(\bar{S})(S-\bar{S}) + 0.5\varphi''(\bar{S})(S-\bar{S})^2 + \ldots$ Integration then gives $\sigma^2 \propto \gamma$.

The saturation regions where the second term is significant (has first order with respect to γ) are the regions of high and low water saturations. In these regions the errors in the individual phase mobilities are represented by the sum of two terms. In the intermediate saturation interval (away from residuals) the error is dominated by the first term, which is the error due to inaccuracy in measured fractional flow.

In this region $\left|\Delta\lambda_i(\bar{S})\right| = \lambda_t(\bar{S})\left|\Delta f_i\right| \leq \lambda_t(\bar{S})\gamma, \quad i = w,o.$